Chrysin Promotes Temozolomide-induced Apoptosis by Activating p38 MAPK and Suppressing Akt and ERK1/2 in Human Glioblastoma.

MUHAMAD NOOR KAMARUDIN (muhamadnoor.alfarizal@monash.edu)
Monash University Malaysia

Ishwar Parhar
Monash University Malaysia

Research Article

Keywords: Chrysin, Glioblastoma, Apoptosis, Temozolomide, Adjuvant, Akt

Posted Date: February 16th, 2021

DOI: https://doi.org/10.21203/rs.3.rs-196841/v1

Abstract

Temozolomide (Tmz) faces the challenges of high chemoresistance and high dose leading to various side-effects. Chrysin exhibits anticancer and adjuvant effects in various cancer models. Nevertheless, chrysin's synergistic effect with Tmz against Tmz-sensitive and Tmz-resistant human glioblastoma has never been reported. Chrysin and Tmz reduced the viability of A172 and LN18 in concentration- and time-dependent manner, with chrysin exhibited IC_{50} values lower than Tmz. The combination of chrysin and Tmz enhanced cell death (CI indexes between 0.59–0.98), suggesting synergistic efficacy of chrysin at lower concentrations. Chrysin promoted Tmz-induced phosphatidylserine externalization and depolarization of mitochondrial membrane potential. Chrysin promoted Tmz-induced suppression of pAkt (Ser473) and pERK1/2 (Thr202/Tyr204) while enhanced the phosphorylation of p38 MAPK (Thr180/Tyr182). This further reduced the antiapoptotic proteins (Bcl-2, Bcl-xL, Mcl-1), elevated proapoptotic proteins (Bax, Bad, Bak, PUMA, Noxa), and activated caspase-9 and caspase-3 compared to Tmz treatment alone. Pretreatment with Z-LEHD-FMK and Z-VAD-FMK attenuated apoptosis and restored caspase-9 and − 3 levels. However, pretreatment with Z-IETD-FMK did not suppress the promotion of apoptosis. Collectively, chrysin promotes Tmz-induced apoptosis through p38 MAPK activation and suppression of Akt and ERK1/2. These results suggest chrysin as a potential therapeutic adjuvant to improve Tmz effects in Tmz-sensitive and -resistant GBM.

Introduction

Gliomas represent about 30% of primary brain tumors, which are believed to originate from the supporting glial cells and are generally categorized into low-grade gliomas and high-grade gliomas [1]. Human glioblastoma (GBM) accounts for almost 80% of the high-grade malignant gliomas as the most aggressive phenotype and worst prognosis among all gliomas [2]. GBM tumors are highly proliferative cells that are capable of infiltrating into the surrounding normal brain tissues; thus, the complete surgical resection is unachievable [2,3]. Even with advancements in therapy, to date, there is no effective therapy with significant improvements against GBM in the last years [4–6].

To date, GBM remains incurable, and despite some therapeutic advancement, the prognosis remains unsatisfactory. Tmz is the main chemotherapeutic agent for human GBM since it is capable of crossing the blood-brain barrier (BBB) [7]. Temozolomide (Tmz) is still widely used as the main chemotherapeutic agent for gliomas, particularly in high-grade gliomas, newly diagnosed GBM with some chemotherapeutic use in recurrent gliomas [5,8,9]. Tmz has been used as a standard chemotherapeutic drug because of its lipophilic nature, and it can cross the blood-brain barrier. The efficacy of Tmz in Stupp's regimen is challenged by high acquired GBM tumors resistance that reverses Tmz-induced DNA damage by the O-6-methylguanine-DNA methyltransferase (MGMT), base excision, and mutation of mismatch repair system [7,10]. Moreover, the high infiltrative and invasive nature of GBM and chemoresistance further limits the efficacy of Tmz that eventually results in GBM recurrence and low median survival rate [3,10]. Furthermore, chemotherapeutic drugs lack the capability to target tumor cells exclusively, which causes severe side-

effects such as suppression of the immune system, nausea, bleeding, and hair loss [3,11]. Despite this, Stupp's regimen continues standing as the standard therapy for GBM management, which commonly prolongs median overall survival of 14.6 months from initial diagnosis (Stupp et al., 2009; Kamarudin and Parhar, 2019). Additionally, in both Tmz-sensitive and -resistant GBM models, Tmz is used at a high dose that leads to severe side-effects with neurocognitive and emotional function impairment among patients [10,12,13].

In recent years, clinical practice of cancer therapy includes the coadministration of targeted molecular drugs that act as an adjuvant to potentiate the efficacy of chemotherapeutic drugs by multitargeting cellular pathways, thus improving drug resistance with lesser side effects [14,15]. Additionally, natural products offer great therapeutic advantages as an effective cancer therapy strategy owing to their ability to target various molecular pathways [16]. Flavonoids, a group of compounds, have been shown to confer anticancer, chemopreventive properties, and other pharmacological benefits in numerous preclinical and epidemiological studies [17–19]. Chrysin (5,7-dihydroxyflavone) is a natural flavonoid that is found abundantly in various fruits, plants, mushrooms, as well as honey. More importantly, chrysin holds a therapeutic promise in cancer therapy since it promotes apoptosis, modulates cell cycle, suppresses angiogenesis and tumor metastasis without triggering cytotoxicity in normal cells [18,20]. Nonetheless, its anticancer promotion activity in human GBM, particularly as a potential adjuvant with Tmz, has never been reported.

Taking this into account, and in view of possible employment of the two drugs, chrysin and Tmz combination were conducted to overcome the limitations of Tmz in drug-sensitive and resistant human GBM cells. The present study demonstrates the synergistic potential of chrysin to promote Tmz sensitivity at a lower concentration by inactivating Akt and ERK1/2 while activating p38 MAPK protein, which promotes the intrinsic apoptotic pathway in both types of GBM models.

Results

Chrysin promotes Tmz-induced cytotoxicity in human GBM cells

Exposure of Tmz-sensitive A172 and Tmz-resistant LN18 cell lines to increasing concentration of chrysin (3.125 – 100 μM) or Tmz (31.25 – 1000 μM) led to concentration- and time-dependent decrease in cell viability, with chrysin IC_{50} values of 38.67 ± 2.34 μM (24 h), 19.43 ± 3.12 μM (48 h) and 52.33 ± 2.62 μM (24 h), 31.46 ± 3.16 μM, respectively (Figure 1A - C, Table 1). Moreover, chrysin demonstrated higher cytotoxicity efficacy at significantly lower IC_{50} values (**p<0.01) than Tmz in both cell lines (Figure 1B and D; summarized in Table 1). Chrysin and Tmz combination studies were performed in both cell lines using a series of IC_{50} concentration (A172: Chrysin, 2.5 – 40 μM, Tmz 25 – 100 μM; LN18: Chrysin 3.75 – 60 μM, Tmz 50 – 200 μM). The CI index < 1 indicates the synergistic killing effect of both chrysin and Tmz combination (48 h) in the GBM cells (summarized in Table 2) with normalized isobologram

combination effects depicted in Figure 1E (A172 cells) and 1F (LN18 cells). Using the three best CI indexes (comparison with the single-drug treatment of chrysin and Tmz alone), cytometric cell viability assay was performed since it is a more robust quantitative measure as compared to MTT assay to further illustrate the best synergistic cell death combination for subsequent analysis (Figure 2). In A172 cells (Figure 2A and B), chrysin alone (20 μM) and in combination treatment (chrysin 20 μM, Tmz 50 μM) exhibited significantly higher dead cell population ($^{\#}p<0.05$) compared to Tmz alone (50 μM). In LN18 cells (Figure 2C and BD, only combination treatment (chrysin 30 μM, Tmz 100 μM) demonstrated a higher dead cell population ($^{\#}p<0.05$) significantly different compared to Tmz alone (100 μM). Therefore, the combination of chrysin 20 μM + Tmz 50 μM and chrysin 30 μM, Tmz 100 μM were chosen for the subsequent apoptosis studies for A172 and LN18 cells, respectively.

Table 1
The IC_{50} (μM) of chrysin and Tmz in A172 and LN18 cells at 24 and 48 h. Values are S.E.M from four independent biological experiments (n=4), where $^{**}p<0.01$ are significant against the Tmz-treated group.

	IC_{50} A172 (μM)	IC_{50} LN18 (μM)
24 h		
Chrysin	$38.67 \pm 2.34^{**}$	$52.33 \pm 2.62^{**}$
Tmz	368 ± 11.44	876 ± 14.51
48 h		
Chrysin	$19.43 \pm 3.12^{**}$	$31.46 \pm 3.16^{**}$
Tmz	141 ± 8.51	527 ± 14.87

Table 2

A) CI values for Tmz and Chrysin combination in A172 cells; combination chrysin (5 – 20 μM) and 50 μM Tmz were selected for subsequent analysis based on CI value (in bold).

Tmz (μM)	Chrysin (μM)	CI value
25	2.5	1.15885
25	5	0.89677
25	10	0.90922
25	20	0.9833
25	40	1.55183
50	2.5	1.03685
50	5	0.8198
50	10	0.81212
50	20	0.66827
50	40	0.81217

Table 2
B) CI values for Tmz and Chrysin combination in LN18 cells; combination chrysin (7.5 – 30 μM) and 100 μM Tmz were selected for subsequent analysis based on CI value (in bold).

Tmz (μM)	Chrysin (μM)	CI value
50	3.75	0.7971
50	7.5	0.7207
50	15	0.5775
50	30	0.8812
50	60	1.0078
100	3.75	1.0568
100	7.5	0.4324
100	15	0.5162
100	30	0.6927
100	60	0.5073

Chrysin promotes Tmz-induced externalization of phosphatidylserine

The exposure of A172 and LN18 to Tmz alone (50 and 100 μM, respectively) increased the apoptotic cell population to 23.6% and 18.9%, respectively (Figure 3A-C). Chrysin single treatment (48 h) alone increased the apoptotic cell population to 30.4% and 27.6% in A172 and LN18, respectively (Figure 3A-C). Interestingly, the combination of chrysin (20 μM) and Tmz (50 μM) significantly augmented ($^{\#}p<0.05$) the apoptotic cell death in A172 to 45.7%, as compared to the Tmz-treated group or chrysin-treated group alone. Similarly, in LN18, the combination treatment (chrysin 20 μM + Tmz 100 μM, for 48 h) increased the apoptotic population to 40.3% ($^{\#}p<0.05$), significantly higher as compared to chrysin or Tmz treatment alone. Collectively, the data demonstrated that a combination treatment of Tmz with chrysin could promote apoptosis higher than single drug treatment despite lower Tmz concentration in both cell lines.

Chrysin enhances Tmz-induced depolarization of mitochondrial membrane potential

Both A172 and LN18 untreated cells displayed an abundance of non-depolarized live cells ~ 93% with a small ~ 3% of depolarized-live cells (Figure 4A-C). Tmz at 50 μM and 100 μM induced mitochondrial membrane depolarization of 35% and 25% in A172 ($^{**}p<0.01$) and LN18 ($^{*}p<0.05$) cells, respectively. Chrysin treatment alone at 20 and 30 μM induced mitochondrial membrane depolarization of 36% and 32% in A172 ($^{**}p<0.01$) and LN18 ($^{**}p<0.05$) cells, respectively. However, chrysin addition (20 μM in A172 and 30 μM in LN18) to Tmz (50 μM in A172 and 100 μM in LN18) treatment significantly promoted the induction of mitochondrial membrane depolarization to 54% (A172; $^{**}p<0.01$) and 49% (LN18, $^{**}p<0.01$) as compared to the Tmz-treated group ($^{\#}p<0.05$). The data demonstrates that a combination of chrysin to Tmz treatment is capable of inducing and further promoting mitochondrial apoptosis in both cell lines.

Chrysin improves Tmz-induced increase in pro-apoptotic and reduces in anti-apoptotic protein levels in GBM cells

The promotion of cellular apoptosis is generally regulated by an increase in ratios between proapoptotic and antiapoptotic protein levels that subsequently induce caspase activation. Tmz or chrysin treatment alone reduced the levels of Bcl-2, Bcl-xL, and Mcl-1 in both A172 and LN18 (Figure 5A-C) cells as compared to untreated cells ($^{*}p<0.05$; $^{**}p<0.01$). Moreover, it was noticeable that the reduction of Bcl-xL and Mcl-1 were more consistent and prominent in both cell lines following treatment with chrysin and Tmz combination as compared to single-drug treatment. The reduction in these antiapoptotic protein levels was accompanied by an increase in proapoptotic proteins Bax, Bak, Bad, PUMA, and Noxa (Figure 6A-C) as compared to untreated cells ($^{*}p<0.05$; $^{**}p<0.01$). Furthermore, the increased level of Bad and PUMA were more consistent and prominent in both cell lines following treatment with chrysin and Tmz combination as compared to single-drug treatment. The current data demonstrate that the addition of chrysin (20 μM in A172 and 30 μM in LN18) into Tmz (50 μM in A172 and 100 μM in LN18) treatment significantly ($^{\#}p<0.05$) enhanced the reduction of antiapoptotic proteins but increased proapoptotic protein levels, leading to a more favorable apoptosis condition (Figure 5A-C and Figure 6A-C) compared to Tmz-treatment group in both A172 and LN18 cell lines.

Chrysin augments Tmz-induced apoptosis by activating p38 MAPK while suppressing Akt and ERK1/2 in both Tmz-sensitive and -resistant GBM cells

Tmz and Chrysin treatment alone to A172 and LN18 cells reduced the level of procaspase-9 (Figure7A and B, ($^{*}p<0.05$). A combination of chrysin with Tmz further reduced procaspase-9 levels significantly in both cell lines, compared to untreated and Tmz-treated only groups ($^{**}p<0.01$, $^{\#}p<0.05$). Similarly, Tmz and chrysin treatment alone reduced procaspase-3 levels in both cell lines, which was further reduced in the combination treatment group ($^{\#}p<0.05$). Additionally, the reduction of procaspases was preceded by the inactivation of pAkt (Ser473) phosphorylation level (Figure7A and C) and pERK1/2 (Figure 8A and C),

significantly as compared to control untreated and single-drug treatment. The combination of chrysin and Tmz treatment also induced the activation of phospho-p38 MAPK and significantly increased the phospho-p38 MAPK/p-38 MAPK ratio compared to control untreated and single drug treatment (Figure 8A and B). Chrysin alone and in combination with Tmz significantly reduced the total Akt, p38 MAPK, and ERK1/2 levels in Tmz-sensitive and Tmz-resistant GBM cells (Figure7A and D). Interestingly, pretreatment with either API-2 or UO126 prior to chrysin and Tmz combination further promoted apoptosis in A172 and LN18 cells (Figure 9C). In contrast, pretreatment with SB 202190 to A172 and LN18 cells significantly suppressed apoptosis (Figure 9C). This observation indicates that the activation of p38 MAPK and inactivation of AKT and ERK1/2 are required for apoptosis promotion by chrysin and Tmz combination treatment in both cell lines.

To corroborate the involvement of extrinsic and intrinsic caspase-mediated apoptosis, A172 and LN18 cells were pretreated with either Z-LEHD-FMK (inhibitor of caspase-9), Z-VAD-FMK (inhibitor of caspase-3), or Z-IETD-FMK (inhibitor of caspase-8). The exposure to either Z-LEHD-FMK or Z-VAD-FMK prior to the combination treatment significantly suppressed apoptosis (Figure 9A), as shown by cytometric annexin analysis. This was further corroborated with the sustained level of procaspase-9 and procaspase-3, as shown by Jess analysis (Figure 9B). However, when both A172 and LN18 cells were pretreated with Z-IETD-FMK, the apoptotic cell population was significantly higher in the chrysin and Tmz combination group, indicating that extrinsic apoptosis was not the main caspase-dependent apoptosis in this system (Figure 9C).

Discussion

To date, GBM remains incurable, and despite some therapeutic advancement, the prognosis remains unsatisfactory. Tmz is the only chemotherapeutic drug used in the treatment of human GBM since it is capable of crossing the BBB [7]. Nevertheless, in both Tmz-sensitive and -resistant GBM models, the effective concentration of Tmz used is rather high that leads to severe side-effects with neurocognitive and emotional function impairment among patients [9,11–13]. Moreover, chemoresistance further limits the efficacy of Tmz that eventually results in GBM recurrence and low median survival rate [10].

The active phytochemicals from plants have gained merits as alternative therapeutics for various diseases such as cancer, neurodegenerative diseases, and diabetes with minimal side-effects and toxicity [21–23]. This nutraceutical holds the therapeutic potential against various chronic diseases since they are capable of modulating multifarious signaling pathways that regulate cellular processes [22–24]. More importantly, they are capable of enhancing the efficacy of chemotherapeutic drugs in killing tumor cells by potentiating apoptosis, autophagy, cell cycle arrestment, enhancing the cellular immune response, and further inhibiting angiogenesis, cell motility, and proliferation [25–27]. Therefore, the use of nutraceutical-based drugs that can improve the effectiveness of Tmz at lower concentrations could reduce drug resistance and enhance the programmed cell death of GBM cells with minimal side effects. Chrysin, a natural flavonoid found in various fruits and plants, including honey, possesses chemopreventive,

antiproliferative, antimetastatic, and antineoplastic activities in various cancer models [20]. However, the potential role of chrysin in different GBM models are not fully explored. Various *in vivo* studies have demonstrated oral administration of chrysin ameliorates neurocognitive dysfunction and neuronal cell death in the brain, suggesting its capability to cross the BBB and be potentially used as an agent that may improve Tmz therapeutic efficacy [28,29].

Programmed cell death through apoptosis is a favorable mode of targeting cancer cell death without triggering inflammatory responses or damaging healthy neighboring cells [30,31]. Chrysin addition enhances the low concentration of Tmz-induced intrinsic apoptosis in both drug-sensitive and resistant GBM cells. The addition of Chrysin at 20 and 30 μM significantly promotes apoptotic inducing effects of Tmz at a lower concentration of 50 μM (A172) and 100 μM (LN18), which is relatively lower than the reported studies [10]. Moreover, the CI indexes further confirmed chrysin synergistically enhances Tmz-induced apoptosis in both Tmz-sensitive and -resistant cells without necrosis, as observed in the cytometric analysis. The induction of mitochondrial-mediated apoptosis is preceded by an increase in ratios of proapoptotic and decrease of antiapoptotic proteins. These proteins govern the permeability of the outer mitochondrial matrix either by preserving the mitochondria membrane integrity or promoting its depolarization. The binding of anti-apoptotic proteins such as Bcl-2, Bcl-xL, and Mcl-1 to pro-apoptotic proteins (Bad, PUMA, Noxa) inactivates the latter and further suppresses the action of pro-apoptotic Bak and Bax protein [32,33]. The current study shows that the addition of chrysin to both Tmz-sensitive and -resistant cells promotes the levels of proapoptotic Bad, Bax, Bak, Noxa, and PUMA levels but significantly reduced Bcl-2, Bcl-xL, and Mcl-1 levels and depolarized mitochondrial membrane. This effect was significantly more pronounced in the combination of chrysin and Tmz groups as compared to either Tmz or chrysin treatment alone. It was observed that elevation pro-apoptotic protein Bad and PUMA levels were consistently and significantly higher than the single drug treatment in both A172 and LN18 cells. Additionally, the levels of Bcl-xL and Mcl-1 expression were consistently and significantly lower than the single drug treatment in both cell lines. Thus, this suggest significant modulation of pro-apoptotic Bad and PUMA as well as anti-apoptotic Bcl-xL and Mcl-1 may serve as the main target of proteins by chrysin and Tmz treatment as compared to chrysin or Tmz single treatment.

It is known that Bad binds to Bcl-xL, which prevents apoptosis inhibition, while Noxa binds to Mcl-1 with high affinity resulting in Mcl-1 proteasomal degradation [34]. Additionally, Noxa improves the efficacy of PUMA in mediating p53-dependent apoptosis [35]. PUMA can activate the translocation of Bax and Bak onto the mitochondrial outer membrane resulting in elevated mitochondria permeability transition pores [36]. This causes the release of apoptogenic factors allowing apoptosome and activation of initiator caspases such as caspase-9 [32,37]. In our study, the addition of chrysin to Tmz treatment significantly decreased procaspase-9 levels suggesting its proteolytic conversion into activated caspase-9 by apoptosome. This is further evident by reduced procaspase-3 levels signifying its activation into active cleaved caspase-3 that eventually leads to intracellular proteolysis and GBM cell death. The current study also showed that the addition of either Z-LEHD-FMK or Z-VAD-FMK significantly reversed this observation and abrogated by a high viable cell population in cytometric analysis. Contrary to this, pretreatment with

Z-IETD-FMK did not suppress the promotion of apoptosis in both cell lines. This then corroborated the findings that chrysin enhances Tmz-induced mitochondrial-mediated apoptosis in both Tmz-sensitive and -resistant GBM cells through a caspase-dependent pathway.

One of the major deregulated pathways in GBM is overactivated PI3K-Akt [38,39]. High percentages of GBM tumors demonstrate increase pAkt (ser473) levels, which allow mTROC1 activation that promotes cell survival, proliferation, and cytoskeletal reorganization [38]. Thus, inactivation of Akt has been viewed as a therapeutic approach that sensitizes GBM tumor cells towards apoptosis while reducing the survival ability. The current data support that the addition of chrysin into Tmz leads to the dephosphorylation of Akt (ser473) leading to reduce pAkt/Akt ratio. Additionally, chrysin treatment alone and in combination with Tmz reduced the total Akt protein in both Tmz-sensitive and -resistant GBM cells. This suggests chrysin possesses the ability to suppress the overexpression and inactivation of Akt protein. Additionally, the deregulation of MAPKs signaling has been associated with the suppression of cellular apoptosis and uncontrolled cell proliferation in the tumor [40,41]. The increased phosphorylation of p38 MAPK has been shown to promote apoptosis in cancer cells by inducing the phosphorylation of pro-apoptotic proteins or inhibiting the anti-apoptotic proteins (Blc-2, Bcl-xL, and Mcl-1), which release their inhibition of pro-apoptotic proteins. Likewise, the activation of ERK1/2 can promote the activity of anti-apoptotic proteins, conferring the survival of tumor cells [41–44]. The aberrant ERK1/2 activation can lead to uncontrolled cell proliferation and differentiation, leading to tumorigenesis. Moreover, chrysin has been reported to induce apoptosis, suppression of cell invasion and promote chemotherapeutic drug action by modulating p38 MAPK and ERK1/2 pathways [42–46]. Our current data demonstrate that the combination of chrysin and Tmz leads to the activation of p38 MAPK while suppressing ERK1/2. Additionally, SB 202190 reverses apoptosis while the addition of API-2 and U0126 further increases apoptosis induction by chrysin and Tmz combination, hence, signifying the importance of these proteins by chrysin and Tmz combination treatment that promotes apoptosis in both GBM cells. Although ERK1/2 is known to activate the NOXA protein, while in this current study, the ERK1/2 phosphorylation level was not completely inhibited, which could be responsible for NOXA expression. Moreover, the inhibition of Akt protein can also promote NOXA, as shown in other studies [47,48].

Phytochemicals, particularly, flavonoids are lipophilic, and BBB permeability serves as the main challenge of their therapeutic efficacy in brain-related disorders. Similarly, one particular aspect in appreciating the ability of chrysin as a potential nutraceutical based adjuvant for GBM treatment in combination with Tmz is its capability to cross the BBB. Additionally, its oral bioavailability is of importance because chrysin has poor absorption with rapid metabolites elimination in the intestines [19]. Nevertheless, current technology that encompassed the use of nanoformulation (nanocapsule, nanoparticles), polymeric micelles, and liposomes that encapsulate chrysin may provide improvement in its BBB transmigration and bioavailability [49,50]. Moreover, the use of solid lipid nanoformulation was shown to increase in *vitro* drug release of chrysin to 83.19 % over 72 hours with a pattern biodistribution and stable physicochemical properties that supports the stability of chrysin (in an intact form) to penetrate the BBB [51]. Therefore, future studies may incorporate the use of this innovative delivery system that may improve the chrysin

delivery across BBB in targeting the GBM tumor. Although some phytochemicals may exert toxicity, flavonoids at low concentrations may be safe for human consumption; chrysin's' recommended concentration is 0.5 to 3g [52]. Although at high concentrations, flavonoids can promote oxidation, chrysin, on the other hand, has been reported to suppress vascular endothelium inflammation by suppressing NF-κB signaling and promote vascular endothelium-dependent aortic relaxation through the promotion of NO production, which may be beneficial in both protecting the endothelial BBB while improving chrysin permeability [53,54]. Additionally, chrysin protects organ tissues against a number of toxic agents and drugs, which in the context of this study, highlights its safe and protective use with Tmz that is known to induce myelotoxicity and side-effects in GBM patients [52,55]. Moreover, studies have shown the ability of chrysin to induce anticancer effect (as a single drug) or promote chemotherapeutic drugs such as doxorubicin and cisplatin in other cancer models as well as in GBM [42–44]. Nevertheless, chrysin being a flavonoid, may possess solubility issues when used at high concentrations; thus, combination studies that reflect the ability of chrysin to be used at lower concentrations with a chemotherapeutic drug may provide some advantages in this situation. Furthermore, chrysin has been shown to be protective of vascular endothelial and endothelial BBB while not exerting toxicity on normal cells [18,53,54,56]. Additionally, the use of nanocarrier confers various advantages for chrysin utilization, delivery to the targeted tumor site, and efficient BBB penetration, particularly in GBM. Taking this into account, chrysin should be considered as a potential nutraceutical adjuvant in promoting the current efficacy of Tmz in GBM studies. However, since the current study focuses on the promotion of Tmz-induced apoptosis, future studies on other anticancer effects such as cell cycle arrestment, autophagic cell death, and suppression of GBM motility should be investigated. Additionally, future studies should also investigate the capability of chrysin to enhance Tmz effects in GBM cells via other signaling pathways that are commonly deregulated in GBM models. Additionally, future animal studies are also warranted to further validate the capability of chrysin as a potential adjuvant of Tmz.

In conclusion, the current study shows that chrysin possesses the ability to promote a low concentration of Tmz-induced cell death via apoptosis induction in both drug-sensitive and resistant GBM cells. Chrysin enhances Tmz-induced p38 MAPK activation and Akt and ERK1/2 inactivation, which elevates proapoptotic and reduces antiapoptotic proteins that promote Bax and Bak translocation to permeabilize the mitochondrial membrane. This enhanced the mitochondrial membrane potential depolarization and led initiator caspase-9 activation and subsequent caspase-3 activation in both GBM cells (Fig. 9D). Therefore, it is noteworthy that chrysin can serve as a potential adjuvant of Tmz in GBM, irrespective of the Tmz resistant status through induction of apoptosis. Nevertheless, future pharmacokinetics and animal studies are still required for chrysin to be validated and potentially be developed to magnify the therapeutic efficacy of Tmz in human GBM cells.

Materials And Methods

Cell culture and reagents

Human GBM A172 (CRL-1620, passage 12 – 22) and LN18 (CRL-2610, passage 539 – 548) cell lines were purchased from the American Type Culture Collection (Manassas, VA, USA). Both cell lines were cultured in complete Dulbecco's Modified Eagle's medium (DMEM) with 10% v/v FBS and 1% antibiotic-antimycotic solution (Gibco®, Thermo Fisher Scientific, USA). The cells were cultured in a humidified incubator (5% CO_2, at 37°C) and routinely subcultured upon reaching 70-80% confluency. TrypLE™ solution (Gibco® Life technologies, Denmark) was used for cell detachment and harvesting. Cells that were subjected to vehicle alone (DMEM, DMSO ≤ 0.5% v/v) were used as the control group. Flow cytometric analysis was done using MUSE™ Cell Analyzer, and the cytometry kits were acquired from Luminex, Austin, USA.

Drugs preparation

Both chrysin and temozolomide (Tmz; as positive control) with purity > 99% were purchased from Sigma Aldrich, USA, while Z-VAD-FMK (>98%), Z-IETD-FMK (>98%), and Z-LEHD-FMK (>98%) were purchased from Enzo Life Sciences, NY, USA. Chrysin was prepared by diluting with DMSO at a stock concentration of 40 mM, while Tmz was prepared at a stock concentration of 140 mM. Z-VAD-FMK was dissolved with DMSO to a stock concentration of 10 mg/mL while Z-LEHD-FMK and Z-IETD-FMK were supplied as a liquid in DMSO. Triciribine hydrate (API-2), U0126, and SB 202190 were purchased from Sigma Aldrich, USA, and prepared at a stock concentration of 10 mM.

MTT assay

Cell viability was investigated using MTT assay [57] with some modification. A total of 5000 viable cells per well were seeded into 96-well plates and incubated overnight. Since several studies have reported different effective range of concentrations for chrysin and for Tmz, therefore, the cells were subjected to treatment with increasing concentration of chrysin (3.125 - 100 µM) or Tmz (31.25 - 1000 µM) for 24 – 48 h. Upon completion of treatment, MTT solution was added (20 µL, 5 mg/mL) (Sigma Aldrich, USA) and left in the CO_2 incubator for 4 h. The media was aspirated, and 150 µL of DMSO (Merck Millipore, Mass., USA) was added to solubilize the formazan salts. The absorbance readings were taken using TECAN Infinite 200 Pro microplate reader (at 570 nm with reference wavelength 650 nm). Following IC_{50} determination, a series of chrysin and Tmz combination treatment was tested, and the synergistic relationship was determined based on the combination index (CI) determined using Compusyn software. The percentage of viable cells was determined by the following equation:

Percentage of viable cells = (Absorbance of treated cells/Absorbance of control cells) x 100%

Synergistic evaluation of chrysin and Tmz Cytotoxicity

The combination effects of chrysin and Tmz was evaluated using the median-effect principle [58]. The A172 and LN18 cells were treated with a series of chrysin (μM) and Tmz combination (IC_{50} concentration range and below) for 48 h and subjected to MTT analysis. The GBM cells were subjected to the combination treatment of 20 μL chrysin (0 - 60 μM) and 20 μL Tmz (0 - 600 μM) for 48 hours, which was based on IC_{50} of each chrysin and Tmz in A172 and LN18 cell lines. These concentrations were selected based on the concentrations that are equal or slightly higher than the known IC_{50} (and lower) of single treatment for each cell line, and therefore, different range of chrysin and Tmz concentrations were investigated throughout this analysis. The use of this range of concentration will demonstrate the ability of combination between chrysin and Tmz at IC_{50} concentration or lower, which may result in cytotoxicity promotion that is higher than single-drug treatment. The combination of chrysin and Tmz was analyzed using Compusyn software based on the fraction of affected cells to generate CI values, which determine synergistic, additive, or antagonistic interaction and normalized isobologram. The CI value for each of the combination treatment was determined using the formula: (D1/Dx1) + (D2/Dx2) + (D1D2/DxlDx2). The Dx1 and Dx2 are the concentration of drug 1 and drug 2, which are required to induce an effect of X percentage. The D1 and D2 represent the combination of the concentration of drugs 1 and 2 required to induce a similar effect. The calculated CI values which are less than 1 indicate synergism. In contrast, CI values equal to 1 and greater than 1 represent the additive and antagonistic effect, respectively.

Determination of cytometric cell viability

To better illustrate the cytotoxicity efficacy of single and combination treatments on GBM cells, cytometric cell viability assay was performed using the Muse™ Cell Viability Kit (Luminex, Austin, USA). This is a more sensitive fluorescent-based-assay as compared to MTT assay, which is based on the reduction of viable mitochondrial dehydrogenase enzymes. The GBM cells were seeded in 60 mm² culture dishes (1×10^6 cells/mL), left to adhere overnight and subjected to either chrysin alone (5 - 20 μM (A172); 10 - 30 μM (LN18), Tmz alone (100 μM (A172); 200 μM (LN18)) or in a combination of chrysin and Tmz (5 - 20 μM + 100 μM (A172); 10 - 30 μM + 200 μM (LN18)). Following this, the cells were carefully rinsed with cold PBS, collected by centrifugation at 1000 rpm (5 min), and resuspended with D-PBS. Cell suspensions (50 μL) were stained with 450 μL Count & Viability Reagent and incubated for 10 min. The cells were then analyzed using Muse™ Cell Analyzer (Luminex, Austin, USA).

Cytometric measurement of apoptosis

Apoptosis induction in both A172 and LN18 cells were detected using Muse™ Annexin V & Dead Cell Assay (Luminex, Austin, USA). The kit utilizes Annexin V to detect externalized phosphatidylserine and 7-AAD that stains the dead cells. In short, the cells (1×10^6 cells/mL) were seeded in 60 mm² culture dishes, left to adhere overnight, and subjected with either chrysin alone (20 μM (A172); 30 μM (LN18), Tmz alone (100 μM (A172); 200 μM (LN18)) or combination of chrysin and Tmz (20 μM + 100 μM (A172); 30 μM + 200 μM (LN18)). After incubation, the cells were gently rinsed with cold PBS, collected by centrifugation

at 1000 rpm (5 min), and resuspended in FBS (1% solution). The cells were stained with Muse™ Annexin V & Dead Cell Reagent (100 µL) and kept in the dark for 20 min. The apoptotic and necrotic cells were observed were by flow cytometry (Muse™ Cell Analyzer, Luminex, Austin, USA) and analyzed with quadrant statistics. To further validate the involvement of caspases and key protein signaling, each GBM cell line was pretreated with pharmacological inhibitors (Z-VAD-FMK (5 µM), Z-IETD-FMK (2 µM), Z-LEHD-FMK (2 µM), API-2 (10 µM), U0126 (10 µM), and SB202190 (10 µM)) prior to chrysin and Tmz combination treatment for 2 h. Following this, the GBM cells were subjected to Annexin analysis.

Mitochondria membrane potential measurement

To determine if the combination treatment promotes apoptosis via an intrinsic pathway, depolarization of mitochondria membrane potential was investigated since it is an early indicator of mitochondrial-mediated intrinsic apoptosis. Depolarization of mitochondria membrane potential following was detected using Muse™ MitoPotential Kit (Luminex, Austin, USA). Similar to annexin measurement, the cells were seeded (1×10^6 cells/mL) and subjected to either chrysin alone (20 µM (A172); 30 µM (LN18), Tmz alone (100 µM (A172); 200 µM (LN18)) or combination of chrysin and Tmz (20 µM + 100 µM (A172); 30 µM + 200 µM (LN18)). Following this, cells were carefully rinsed with cold PBS and centrifuged at 1000 rpm (5 min). The cells (100 µL) were stained with 95 µL Muse™ MitoPotential reagent prepared in 1x Assay buffer and incubated (20 min) at 37 °C. Next, 5 µL of 7-AAD dye was added, and cells were incubated for 5 min before subjected to Muse™ Cell Analyzer (Luminex, Austin, USA).

JESS Simple Western analysis

To further substantiate the promotion of intrinsic apoptosis, the levels of major proapoptotic and antiapoptotic proteins involved in mitochondrial-mediated apoptosis were evaluated. JESS Simple Western (Santa Clara, CA, USA) was employed to detect key apoptotic proteins following treatment with chrysin and Tmz in both A172 and LN18 cells based on the manufacturer's protocol. A total of 1×10^6 cells/mL of either A172 or LN18 cells were plated on 60 mm^2 culture dishes and subjected to a similar treatment paradigm comprising of chrysin and Tmz alone or in combination. The GBM cells were carefully collected by rinsing with PBS and harvested by centrifugation at 1000 rpm. The cell pellets were subjected to RIPA buffer (Nakalai, Japan) and centrifuged at 14 000 rpm (20 min, 4 °C). Bradford Protein Assay Kit (Bio-Rad, Hercules, CA, USA) was employed to determine the concentration of protein in each sample. A total of 2 µg protein lysate was mixed with a mastermix reagent to achieve a final concentration of 1x sample buffer that was prepared with chemiluminescent molecular weight markers and dithiothreitol (40 mM). The mixture was denatured by heating for 5 min at 95 °C. Biotinylated ladder (5 µL) and each of the sample lysate (5 µL) were loaded into the well plate. The target proteins were immune-probed with primary antibodies (10 µL) diluted using an antibody diluent at a 1:25 or 1:50 ratio (anti-β-actin, anti-Bcl-2, anti-Bcl-xL, anti-Mcl-1, anti-Bax, anti-Bak, anti-Bad, anti-PUMA, anti-Noxa, anti-pro-caspase 9, anti-procaspase 3, anti-panAkt, anti-pAkt(Ser473), anti-p44/42 MAPK (Erk1/2), Phospho-

p44/42 MAPK (Erk1/2) (Thr202/Tyr204), p38 MAPK, and Phospho-p38 MAPK (Thr180/Tyr182) (Cell Signaling Technology, MA, USA) followed by HRP-conjugated secondary antibodies (10 µL). GAPDH was used as the housekeeping protein and all the samples loaded were normalized using protein normalization reagent. The bands were visualized by the addition of luminol peroxidase. The digital image density was analyzed using Compass software (Protein Simple), where the detected proteins were quantified by the signal/peak intensity.

Statistical analysis

The experiments were conducted in triplicate, and data were presented in means ± standard error (S.E.). Student's t-test and Mann's Whitney were used for the determination of statistical significance (p values <0.05 or $^{**}p$ values <0.01) and differences between control untreated and treated groups. Statistical analyses between treated groups were determined using one-way ANOVA and Dunnett's test (significant $^{\#}p$ values <0.05). Statistical analysis was performed using GraphPad Prism 5.0 (GraphPad software).

Abbreviations

BBB, Blood-brain barrier; CI, combination index; DMEM, *Dulbecco's Modified Eagle's medium;* GBM, Glioblastoma; MGMT, O-6-methylguanine-DNA methyltransferase; Tmz, Temozolomide

Declarations

Conflict of Interest

The authors declare that the research was conducted in the absence of any commercial or financial relationships that could be construed as a potential conflict of interest.

Author Contributions

MNAK: Conceptualization, Methodology, Investigation, Writing – original draft, visualization, data analysis, Writing – review & editing.

IP: Conceptualization, Project administration, Funding acquisition, Writing – review & editing.

All authors read and approved the final manuscript.

Funding

The authors would like to thank Brain Research Institute Monash Sunway (BRIMS), Jeffrey Cheah School of Medicine and Health Sciences, Monash University Malaysia for the research funding.

Acknowledgments

The authors would like to thank Brain Research Institute Monash Sunway (BRIMS), Jeffrey Cheah School of Medicine and Health Sciences, Monash University Malaysia for the research funding.

References

1. Llaguno, S. R. A. & Parada, L. F. Cell of origin of glioma: biological and clinical implications. *British Journal of Cancer.* **115**, 1445–1450 (2016).
2. Vigneswaran, K., Neill, S. & Hadjipanayis, C. G. Beyond the World Health Organization grading of infiltrating gliomas: advances in the molecular genetics of glioma classification.*Annals of Translational Medicine***3** (2015).
3. Kamarudin, M. N. & Parhar, I. Emerging therapeutic potential of anti-psychotic drugs in the management of human glioma: a comprehensive review. *Oncotarget.* **10**, 3952 (2019).
4. Lee, D. H., Ryu, H. W., Won, H. R. & Kwon, S. H. Advances in epigenetic glioblastoma therapy. *Oncotarget.* **8**, 18577 (2017).
5. Lukas, R. V. *et al.* Newly diagnosed glioblastoma: a review on clinical management. *Oncology (Williston Park, NY).* **33**, 91 (2019).
6. Rick, J., Chandra, A. & Aghi, M. K. Tumor treating fields: a new approach to glioblastoma therapy. *Journal of Neuro-Oncology.* **137**, 447–453 (2018).
7. Stupp, R. *et al.* Effects of radiotherapy with concomitant and adjuvant temozolomide versus radiotherapy alone on survival in glioblastoma in a randomised phase III study: 5-year analysis of the EORTC-NCIC trial. *Lancet Oncol.* **10**, 459–466 (2009).
8. Glas, M. *et al.* Long-term survival of glioblastoma patients treated with radiotherapy and lomustine plus temozolomide. *Journal of Clinical Oncology.* **27**, 1257–1261 (2009).
9. Wick, A. *et al.* Efficacy and tolerability of temozolomide in an alternating weekly regimen in patients with recurrent glioma. *Journal of Clinical Oncology.* **25**, 3357–3361 (2007).
10. Lee, S. Y. Temozolomide resistance in glioblastoma multiforme. *Genes & Diseases.* **3**, 198–210 (2016).
11. Niewald, M. *et al.* Toxicity after radiochemotherapy for glioblastoma using temozolomide-a retrospective evaluation. *Radiat. Oncol.* **6**, 141 (2011).
12. Lombardi, G. *et al.* Quality of Life Perception, Cognitive Function, and Psychological Status in a Real-world Population of Glioblastoma Patients Treated With Radiotherapy and Temozolomide. *American Journal of Clinical Oncology.* **41**, 1263–1271 (2018).
13. Macdonald, D. R., Kiebert, G., Prados, M., Yung, A. & Olson, J. Benefit of temozolomide compared to procarbazine in treatment of glioblastoma multiforme at first relapse: effect on neurological functioning, performance status, and health related quality of life. *Cancer Invest.* **23**, 138–144 (2005).

14. Chio, C. C. *et al.* Honokiol enhances temozolomide-induced apoptotic insults to malignant glioma cells via an intrinsic mitochondrion-dependent pathway. *Phytomedicine.* **49**, 41–51 (2018).
15. Fratantonio, D. *et al.* Curcumin potentiates the antitumor activity of Paclitaxel in rat glioma C6 cells. *Phytomedicine.* **55**, 23–30 https://doi.org/10.1016/j.phymed.2018.08.009 (2019).
16. Lin, S. R. *et al.* Natural compounds as potential adjuvants to cancer therapy: Preclinical evidence. *British Journal of Pharmacology.* **177**, 1409–1423 (2020).
17. Abotaleb, M. *et al.* Flavonoids in cancer and apoptosis. *Cancers.* **11**, 28 (2019).
18. Kasala, E. R., Bodduluru, L. N., Madana, R. M., Gogoi, R. & Barua, C. C. Chemopreventive and therapeutic potential of chrysin in cancer: mechanistic perspectives. *Toxicol. Lett.* **233**, 214–225 (2015).
19. Mani, R., Natesan, V. & Chrysin Sources, beneficial pharmacological activities, and molecular mechanism of action. *Phytochemistry.* **145**, 187–196 (2018).
20. Mehdi, S. *et al.* A promising anticancer agent its Current trends and future Perspectives. *Eur Exp Biol.* **8**, 16 (2018).
21. Costa, C. *et al.* Current evidence on the effect of dietary polyphenols intake on chronic diseases. *Food and Chemical Toxicology.* **110**, 286–299 (2017).
22. Nabavi, M., Daglia, M. & S. & Phytochemicals for Human Diseases: An Update. *Curr. Drug Targets.* **18**, 1467–1467 (2017).
23. Sharma, S. & Naura, A. S. Potential of phytochemicals as immune-regulatory compounds in atopic diseases: A review. *Biochem. Pharmacol.* **173**, 113790 (2020).
24. Zhang, H. & Tsao, R. Dietary polyphenols, oxidative stress and antioxidant and anti-inflammatory effects. *Current Opinion in Food Science.* **8**, 33–42 (2016).
25. Gajbhiye, R. L., Mahato, S. K., Achari, A., Jaisankar, P. & Ravichandiran, V. in Bioactive Natural Products for the Management of Cancer: from Bench to Bedside 91–109(Springer, 2019).
26. Link, A., Balaguer, F. & Goel, A. Cancer chemoprevention by dietary polyphenols: promising role for epigenetics. *Biochem. Pharmacol.* **80**, 1771–1792 (2010).
27. Ruiz, R. B. & Hernández, P. S. Cancer chemoprevention by dietary phytochemicals: Epidemiological evidence. *Maturitas.* **94**, 13–19 (2016).
28. Angelopoulou, E., Pyrgelis, E. S. & Piperi, C. Neuroprotective potential of chrysin in Parkinson's disease: Molecular mechanisms and clinical implications. *Neurochem. Int.* **132**, 104612 (2020).
29. Mani, R., Natesan, V. & Arumugam, R. Neuroprotective effect of chrysin on hyperammonemia mediated neuroinflammatory responses and altered expression of astrocytic protein in the hippocampus. *Biomed. Pharmacother.* **88**, 762–769 (2017).
30. D'Arcy, M. S. Cell death: a review of the major forms of apoptosis, necrosis and autophagy. *Cell. Biol. Int.* **43**, 582–592 (2019).
31. Hengartner, M. O. The biochemistry of apoptosis. *Nature.* **407**, 770–776 (2000).

32. Cory, S., Roberts, A. W., Colman, P. M. & Adams, J. M. Targeting BCL-2-like proteins to kill cancer cells. *Trends in Cancer.* **2**, 443–460 (2016).
33. Campbell, K. J. & Tait, S. W. Targeting BCL-2 regulated apoptosis in cancer. *Open Ciology.* **8**, 180002 (2018).
34. Levy, M. A. & Claxton, D. F. Therapeutic inhibition of BCL-2 and related family members. *Expert Opinion on Investigational Drugs.* **26**, 293–301 (2017).
35. Guikema, J. E., Amiot, M. & Eldering, E. Exploiting the pro-apoptotic function of NOXA as a therapeutic modality in cancer. *Expert Opinion on Therapeutic Targets.* **21**, 767–779 (2017).
36. Peña-Blanco, A., García-Sáez, A. J. & Bax Bak and beyond—mitochondrial performance in apoptosis. *The FEBS Journal.* **285**, 416–431 (2018).
37. Zhang, L., Li, J. & Xu, W. A review of the role of Puma, Noxa and Bim in the tumorigenesis, therapy and drug resistance of chronic lymphocytic leukemia. *Cancer Gene Ther.* **20**, 1–7 (2013).
38. Li, X. *et al.* PI3K/Akt/mTOR signaling pathway and targeted therapy for glioblastoma. *Oncotarget.* **7**, 33440 (2016).
39. Lo, H. W. EGFR-targeted therapy in malignant glioma: novel aspects and mechanisms of drug resistance. *Current MolecularPpharmacology.* **3**, 37–52 (2010).
40. Wang, R. *et al.* Evodiamine activates cellular apoptosis through suppressing PI3K/AKT and activating MAPK in glioma. *OncoTargets and Therapy.* **11**, 1183 (2018).
41. Yue, J. & López, J. M. Understanding MAPK signaling pathways in apoptosis. *International Journal of Molecular Sciences.* **21**, 2346 (2020).
42. Wang, J. *et al.* Chrysin suppresses proliferation, migration, and invasion in glioblastoma cell lines via mediating the ERK/Nrf2 signaling pathway. *Drug Design, Development and Therapy.* **12**, 721 (2018).
43. Gao, A. M., Ke, Z. P., Shi, F., Sun, G. C. & Chen, H. Chrysin enhances sensitivity of BEL-7402/ADM cells to doxorubicin by suppressing PI3K/Akt/Nrf2 and ERK/Nrf2 pathway. *Chemico-Biol. Interact.* **206**, 100–108 (2013).
44. Li, X. *et al.* Combination of chrysin and cisplatin promotes the apoptosis of Hep G2 cells by up-regulating p53. *Chemico-Biol. Interact.* **232**, 12–20 (2015).
45. Park, W., Park, S., Lim, W. & Song, G. Chrysin disrupts intracellular homeostasis through mitochondria-mediated cell death in human choriocarcinoma cells. *Biochemical and Biophysical Research Communications.* **503**, 3155–3161 (2018).
46. Ryu, S., Lim, W., Bazer, F. W. & Song, G. Chrysin induces death of prostate cancer cells by inducing ROS and ER stress. *Journal of Cellular Physiology.* **232**, 3786–3797 (2017).
47. Yan, Y. *et al.* A novel derivative of valepotriate inhibits the PI3K/AKT pathway and causes Noxa-dependent apoptosis in human pancreatic cancer cells. *Acta Pharmacol. Sin.* **41**, 835–842 (2020).
48. Zhan, Y. *et al.* BH3 mimetic ABT-263 enhances the anticancer effects of apigenin in tumor cells with activating EGFR mutation. *Cell & Bioscience.* **9**, 1–18 (2019).

49. Branquinho Andrade, P., Grosso, C., Valentao, P. & Bernardo, J. Flavonoids in neurodegeneration: Limitations and strategies to cross CNS barriers. *Curr. Med. Chem.* **23**, 4151–4174 (2016).
50. Shankar, R., Joshi, M. & Pathak, K. Lipid nanoparticles: A novel approach for brain targeting. *Pharmaceutical Nanotechnology.* **6**, 81–93 (2018).
51. Aishwarya, V. & Sumathi, T. Enhanced blood–brain barrier transmigration using the novel chrysin embedded solid lipid nanoformulation: A salient approach on physico-chemical characterization, pharmacokinetics and biodistribution studies. *Int. J. Pharm. Clin. Res.* **8**, 1574–1582 (2016).
52. Samarghandian, S., Farkhondeh, T. & Azimi-Nezhad, M. Protective effects of chrysin against drugs and toxic agents. *Dose-Response.* **15**, 1559325817711782 (2017).
53. Villar, I. C. *et al.* Endothelial nitric oxide production stimulated by the bioflavonoid chrysin in rat isolated aorta. *Planta Med.* **71**, 829–834 (2005).
54. Zhao, S. *et al.* Chrysin suppresses vascular endothelial inflammation via inhibiting the NF-κB signaling pathway. *Journal of Cardiovascular Pharmacology and Therapeutics.* **24**, 278–287 (2019).
55. Singhal, N., Selva-Nayagam, S. & Brown, M. P. Prolonged and severe myelosuppression in two patients after low-dose temozolomide treatment-case study and review of literature. *Journal of Neuro-oncology.* **85**, 229–230 (2007).
56. Mehdi, S. *et al.* A promising anticancer agent its Current trends and future Perspectives. *Eur. J. Exp. Biol.* **8**, 16 (2018).
57. Goh, B. H., Chan, C. K., Kamarudin, M. N. A. & Abdul Kadir, H. Swietenia macrophylla King induces mitochondrial-mediated apoptosis through p53 upregulation in HCT116 colorectal carcinoma cells. *Journal of Ethnopharmacology.* **153**, 375–385 https://doi.org/10.1016/j.jep.2014.02.036 (2014).
58. Chou, T. C. Theoretical basis, experimental design, and computerized simulation of synergism and antagonism in drug combination studies. *Pharmacol. Rev.* **58**, 621–681 (2006).

Figures

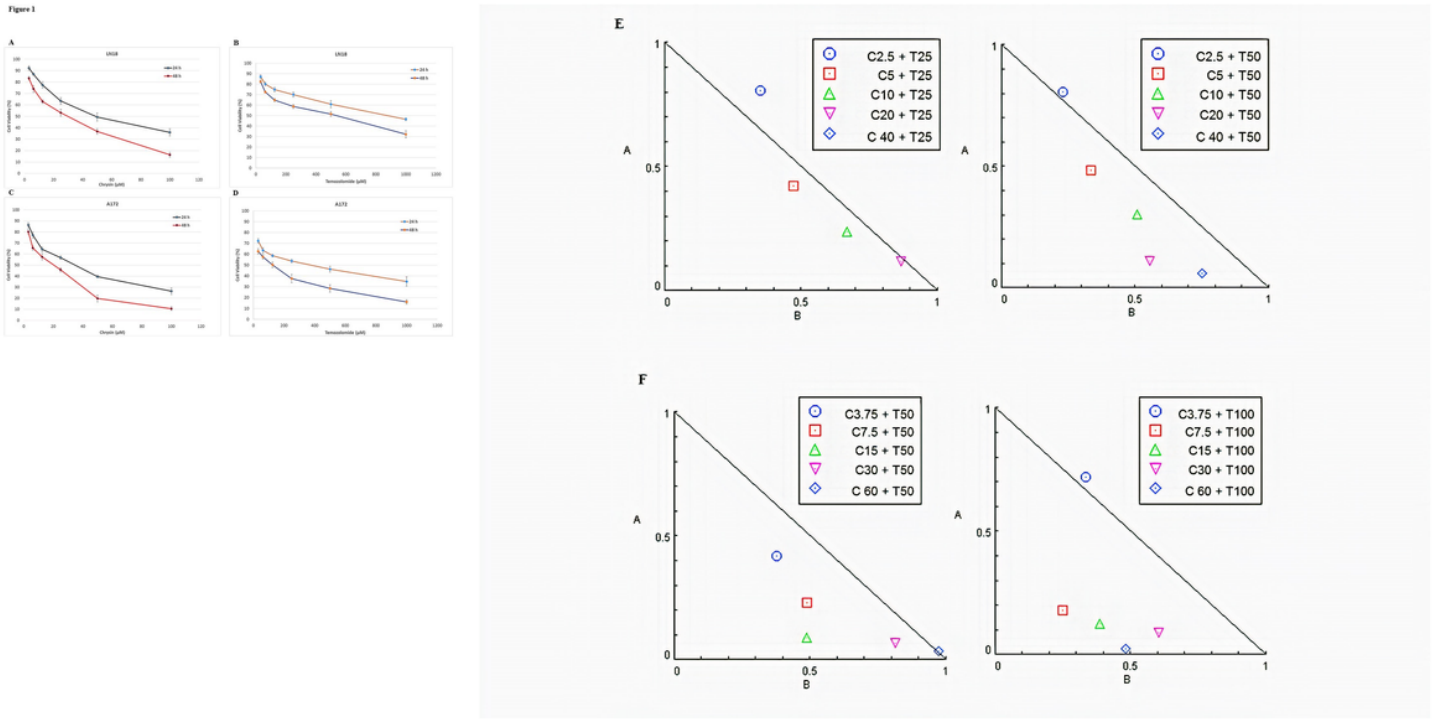

Figure 1

MTT assay. Cells were treated with an increasing concentration of either chrysin 3.125 – 100 μM) or Tmz (31.25 – 1000 μM) for 24 and 48 h. Reduction of LN18 cell viability following treatment with (A) chrysin or (B) Tmz. A172 cell viability following treatment with (C) chrysin or (D) Tmz. (E) Normalized isobologram of A172 cells following combination treatment of chrysin (2.5 - 40 μM) with Tmz (25 and 50 μM). (F) Normalized isobologram of LN18 cells following combination treatment of chrysin (3.75 - 60 μM) with Tmz (50 and 100 μM). Values are means from four independent biological experiments (n=4).

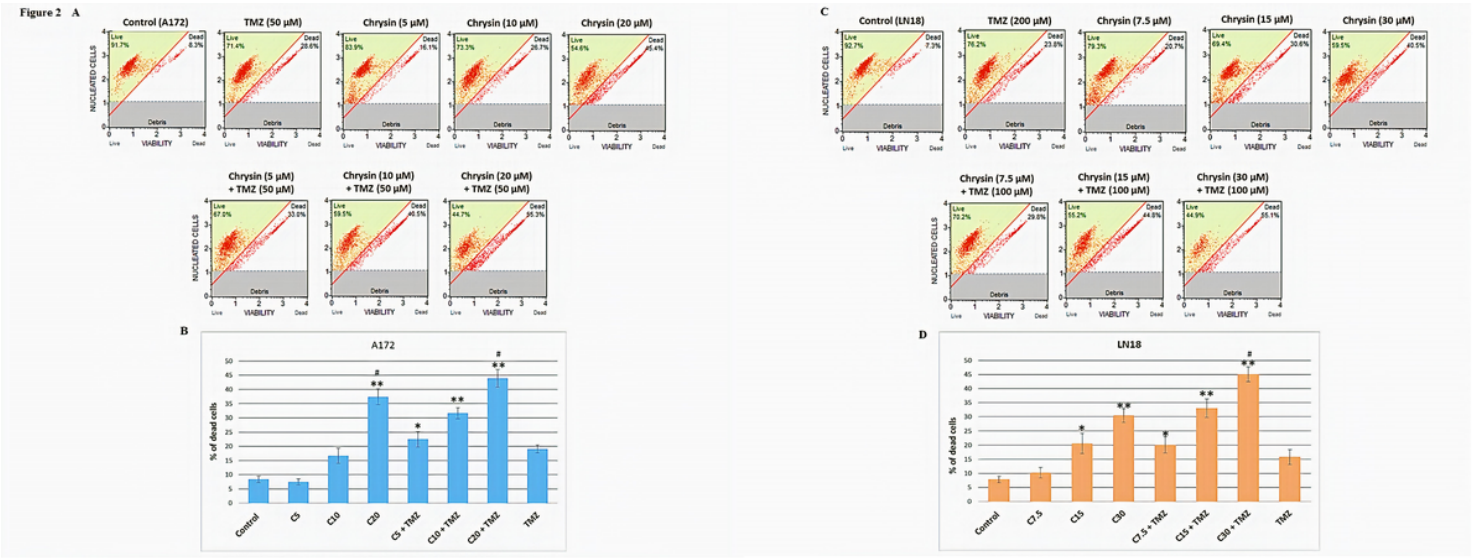

Figure 2

Flow cytometry of viable and dead cells analysis. (A) A172 cell viability following exposure to either chrysin (5 – 20 μM), Tmz (50 μM), or chrysin (5 – 20 μM) + Tmz (50 μM). (B) The bar graph represents the percentage of A172 dead cells. (C) LN18 cell viability following treatment with either chrysin (7.5 – 30 μM), Tmz (100 μM), or chrysin (7.5 – 30 μM) + Tmz (100 μM). (D) The bar graph represents the percentage of LN18 dead cells. Values are S.E.M from three independent biological experiment (n=3), where *p <0.05, **p <0.01 are significant versus control and #p <0.05 is significant against Tmz-treated group.

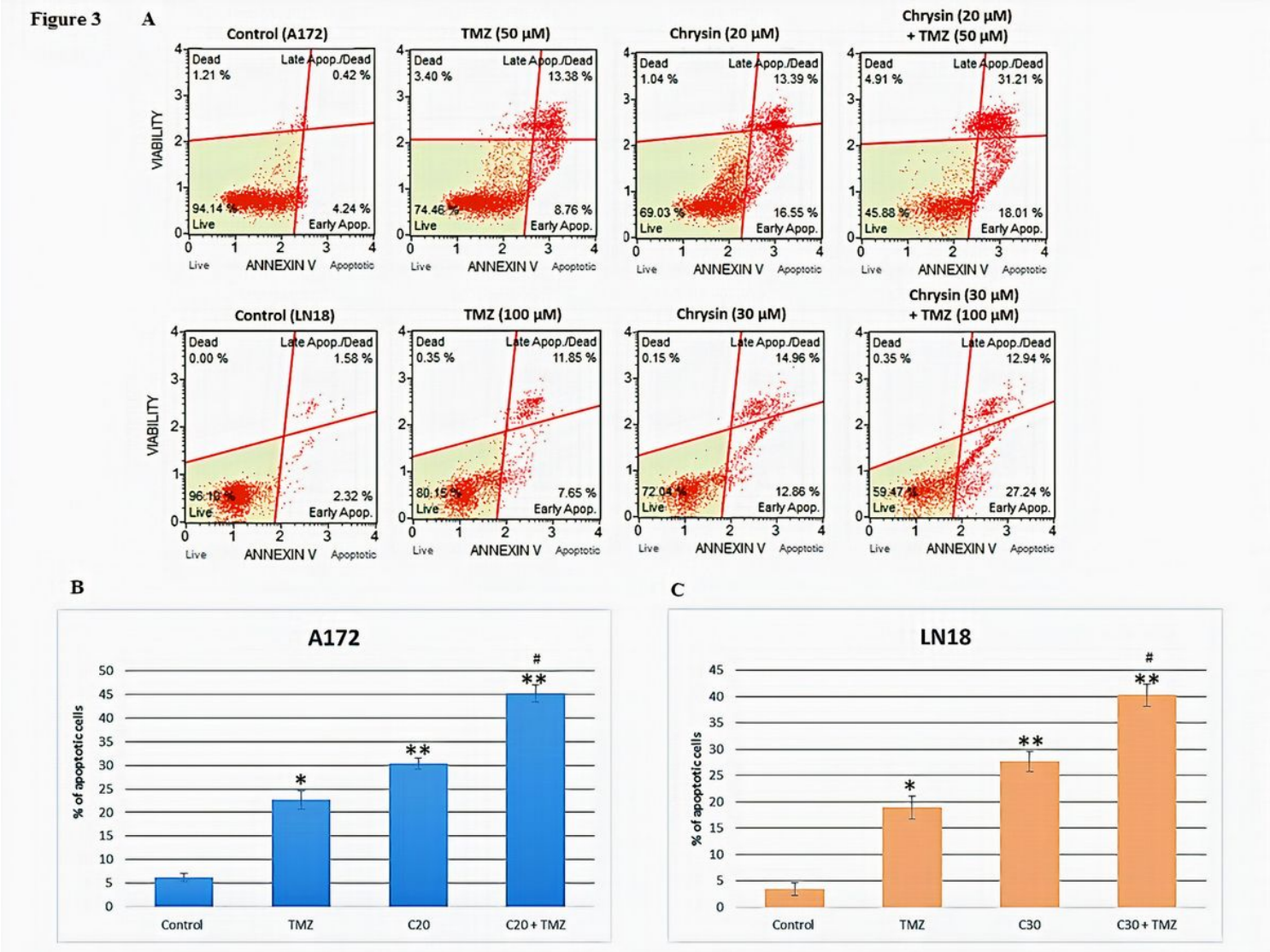

Figure 3

Cytometric apoptotic cell analysis. (A) Dot plot analysis of apoptotic cell population (early and late) following treatment (A172: chrysin (20 μM), Tmz (50 μM) or chrysin (20 μM) + Tmz (50 μM); LN18: chrysin (30 μM), Tmz (100 μM) or chrysin (30 μM) + Tmz (100 μM)) for 48 h. Bar graphs show chrysin or Tmz exposure increased total apoptotic cell population in (B) A172 and (C) LN18 cell lines. The addition of chrysin to Tmz further increased the total apoptotic cell population in both cell lines. Values are S.E.M from three independent biological experiment (n=3), where *p <0.05, **p <0.01 are significant versus control and #p <0.05 is significant against Tmz-treated group.

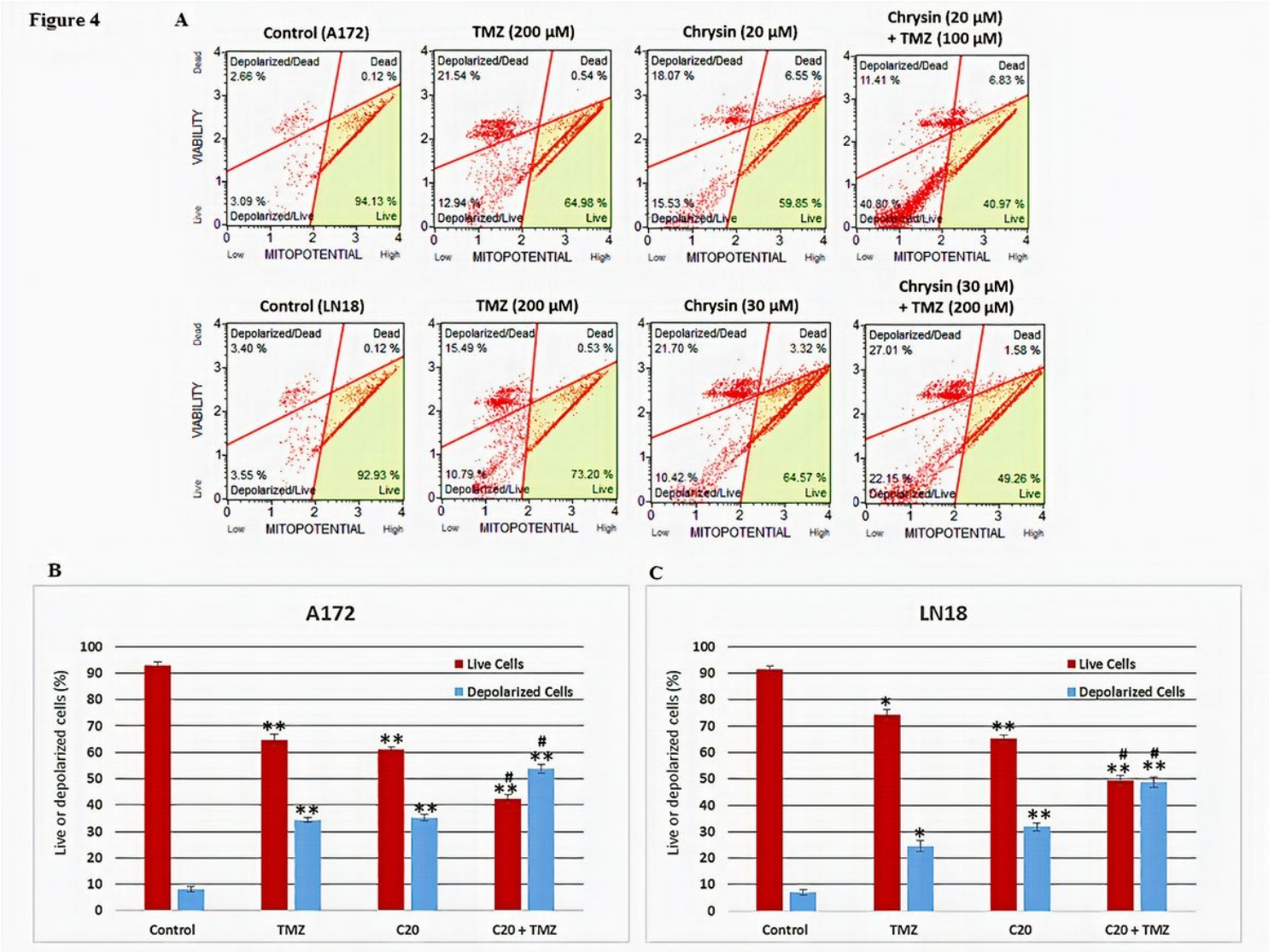

Figure 4

Analysis of mitochondrial membrane depolarization. (A) Dot plot analysis of depolarized mitochondrial cells (live/dead) following treatment (A172: chrysin (20 µM), Tmz (50 µM) or chrysin (20 µM) + Tmz (50 µM); LN18: chrysin (30 µM), Tmz (100 µM) or chrysin (30 µM) + Tmz (100 µM)) for 48 h. Bar graphs show the reduction of live cells and the increase of total depolarized cells in both (B) A172 and (C) LN18 cell lines. Chrysin addition to Tmz treatment further enhanced the depolarization of mitochondrial membrane in both cell lines. Values are S.E.M from three independent biological experiment (n=3), where *p <0.05, **p <0.01 are significant versus control and #p <0.05 is significant against Tmz-treated group.

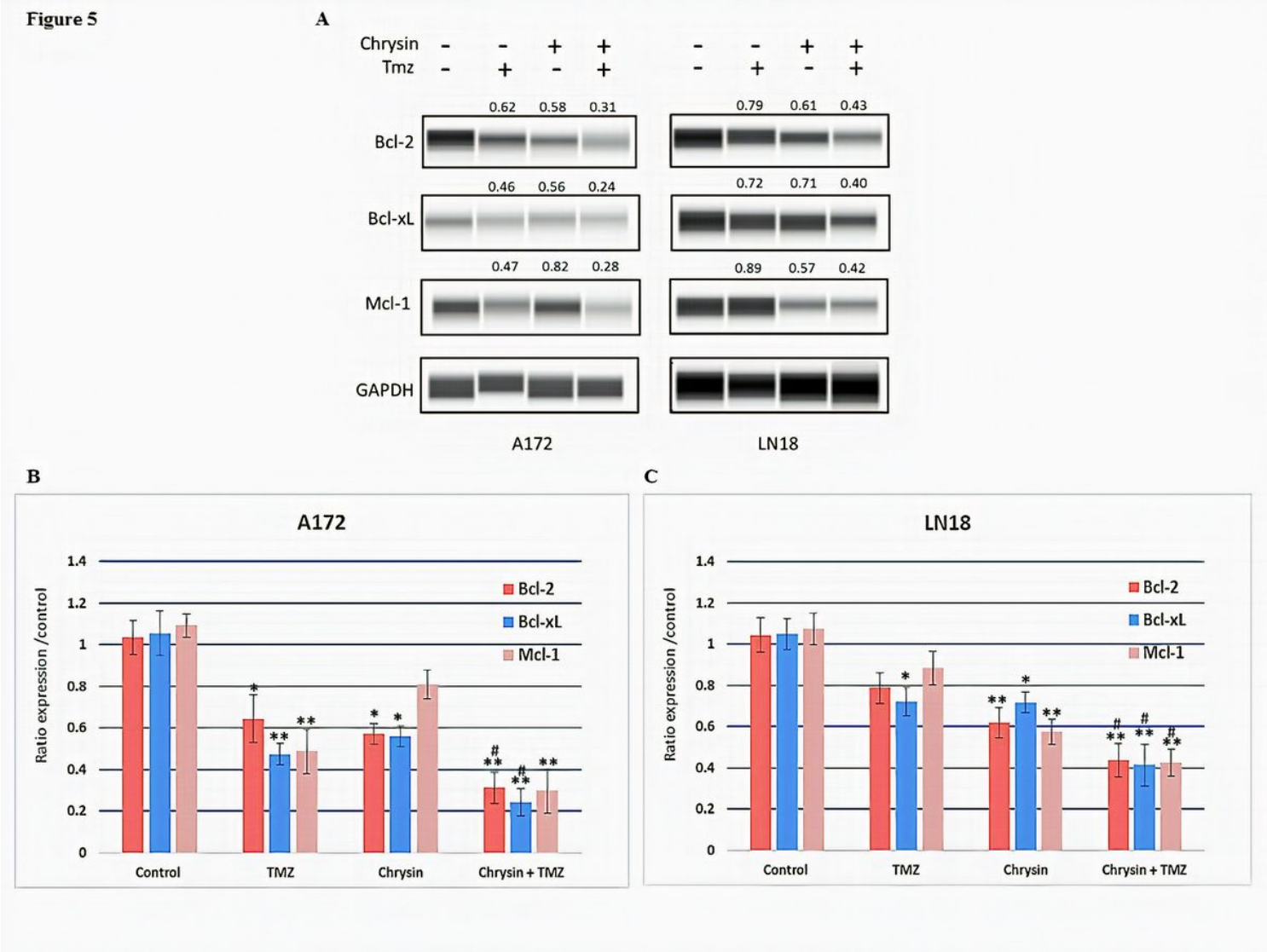

Figure 5

JESS simple western analysis of antiapoptotic proteins. (A) Blot images of Bcl-2, Bcl-xL, and Mcl-1 following treatment (A172: chrysin (20 μM), Tmz (50 μM) or chrysin (20 μM) + Tmz (50 μM); LN18: chrysin (30 μM), Tmz (100 μM) or chrysin (30 μM) + Tmz (100 μM)) for 48 h. Lane 1, control; lane 2, Tmz; lane 3, chrysin; lane 4, chrysin+Tmz. Bar graphs show the reduction of Bcl-2, Bcl-xL, and Mcl-1 protein levels in (B) A172 and (C) LN18 cell lines. Chrysin addition to Tmz further reduced the antiapoptotic protein levels in both cell lines compared to the Tmz-treated group. The JESS image blot was cropped from the whole blot according to the proteins. Values are S.E.M from three independent biological experiment (n=3), where *p <0.05, **p <0.01 are significant versus control and #p <0.05 is significant against Tmz-treated group.

Figure 6

JESS simple western analysis of proapoptotic proteins. (A) Blot images of Bax, Bak, Bad, PUMA, and Noxa following treatment (A172: chrysin (20 μM), Tmz (50 μM) or chrysin (20 μM) + Tmz (50 μM); LN18: chrysin (30 μM), Tmz (100 μM) or chrysin (30 μM) + Tmz (100 μM)) for 48 h. Lane 1, control; lane 2, Tmz; lane 3, chrysin; lane 4, chrysin+Tmz. Bar graphs show the reduction of Bcl-2, Bcl-xL, and Mcl-1 protein levels in (B) A172 and (C) LN18 cell lines. Chrysin addition to Tmz further increased the proapoptotic protein levels in both cell lines compared to the Tmz-treated group. The JESS image blot was cropped from the whole blot according to the proteins. Values are S.E.M from three independent biological experiment (n=3), where *p <0.05, **p <0.01 are significant versus control and #p <0.05 is significant against Tmz-treated group.

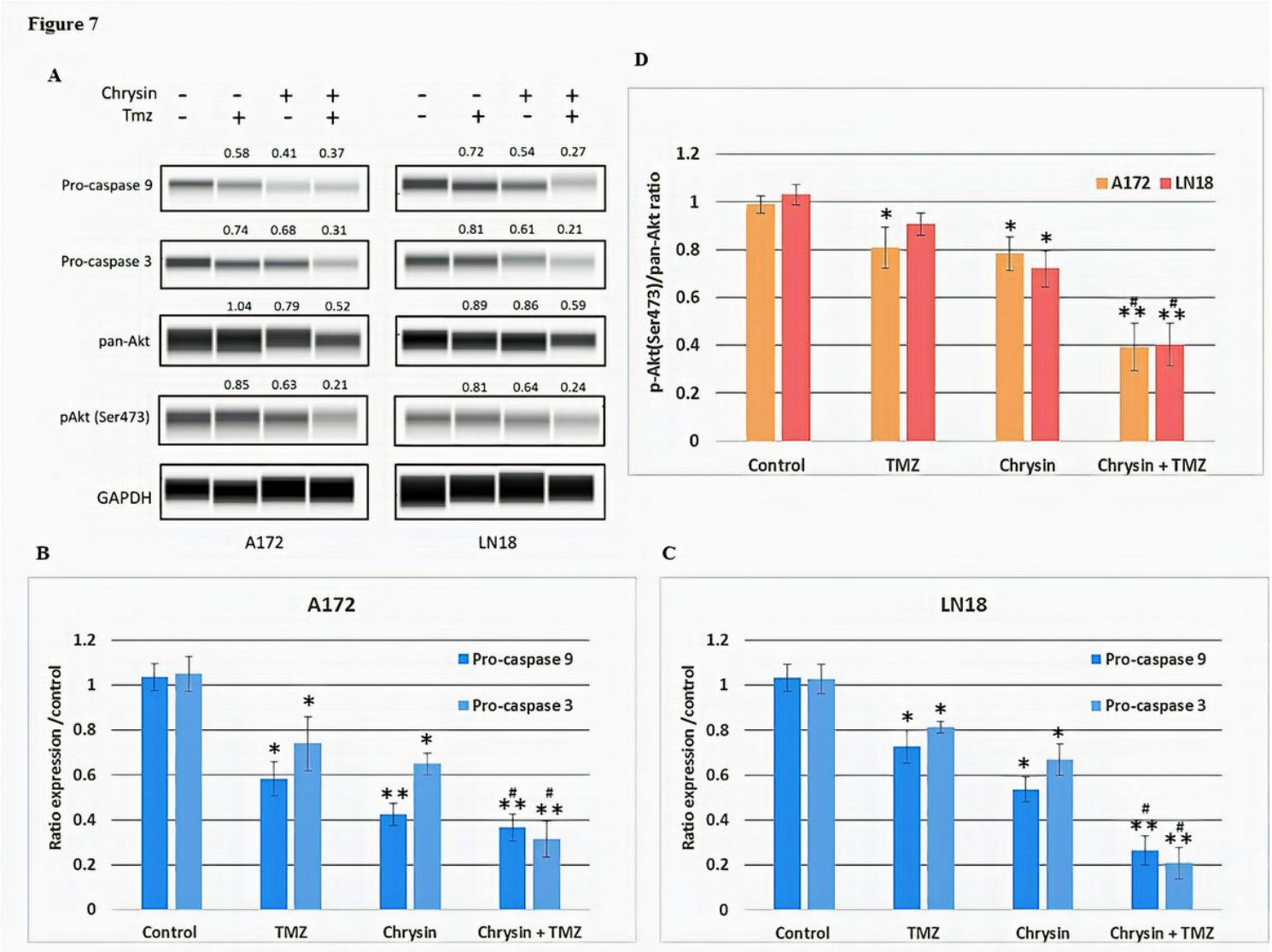

Figure 7

JESS simple western analysis of procaspase-9, procaspase-3, and Akt proteins. (A) Blot images of procaspase-9, procaspase-3, total Akt and pAkt(ser473) proteins following treatment (A172: chrysin (20 μM), Tmz (50 μM) or chrysin (20 μM) + Tmz (50 μM); LN18: chrysin (30 μM), Tmz (100 μM) or chrysin (30 μM) + Tmz (100 μM)).. Lane 1, control; lane 2, Tmz; lane 3, chrysin; lane 4, chrysin+Tmz. Bar graphs show the reduction of procaspase-9 and -3 levels in (B) A172 and (C) LN18 cell lines. (D) The bar graph shows the reduced pAkt/Akt ratios in both A172 and LN18 cells lines. Chrysin addition to Tmz significantly enhanced the reduction of procaspase-9, -3, total Akt, and pAkt levels of protein levels in both cell lines compared to the Tmz-treated group. The JESS image blot was cropped from the whole blot according to the proteins. Values are S.E.M from three independent biological experiment (n=3), where *p <0.05, **p <0.01 are significant versus control and #p <0.05 is significant against Tmz-treated group.

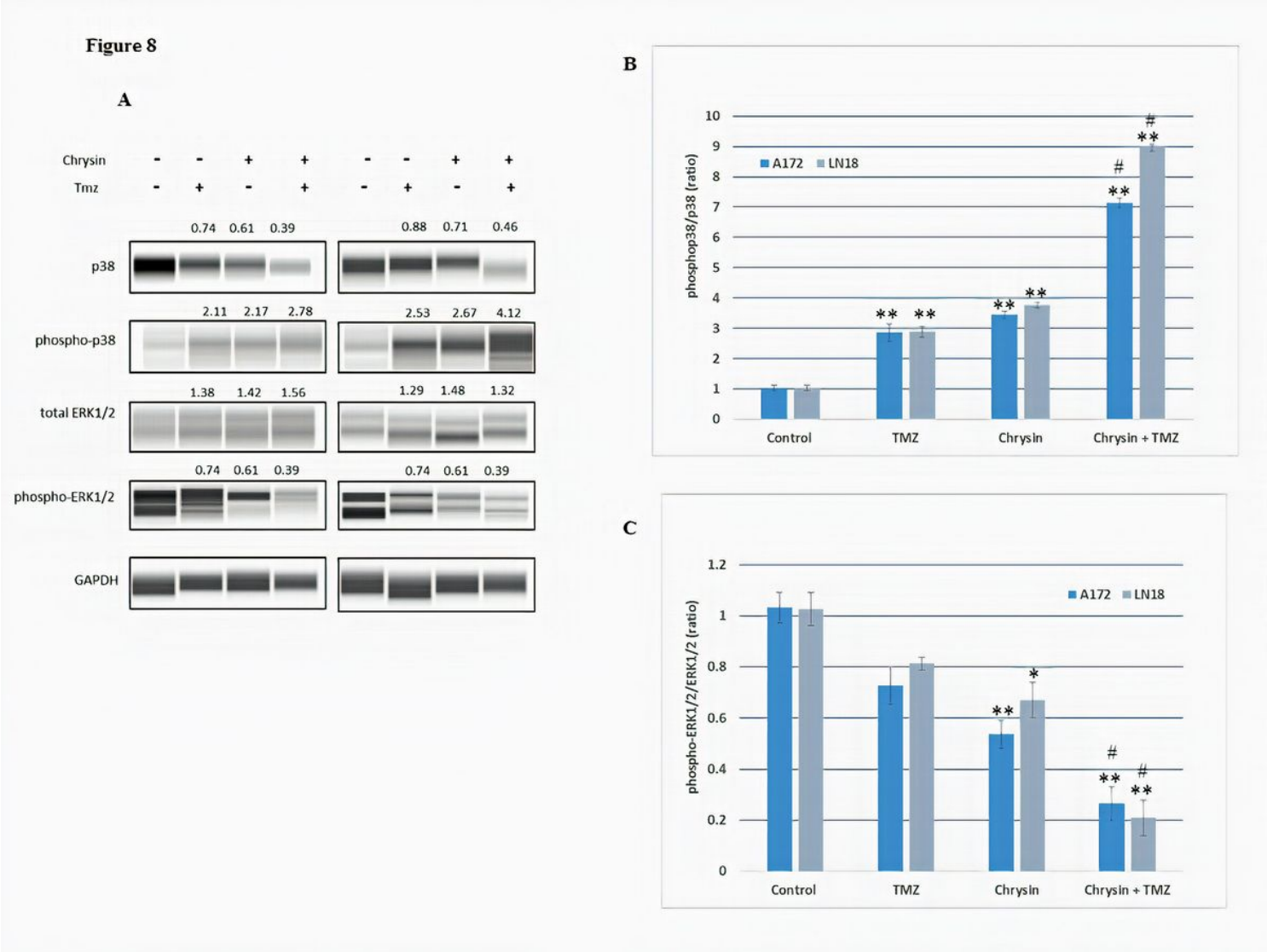

Figure 8

JESS simple western analysis of p38 MAPK and ERK1/2 in A172 and LN18 cells. (A) Blot images of p38 MAPK, phospho-p38 MAPK, ERK1/2, and phospho-ERK1/2 proteins following treatment (A172: chrysin (20 μM), Tmz (50 μM) or chrysin (20 μM) + Tmz (50 μM); LN18: chrysin (30 μM), Tmz (100 μM) or chrysin (30 μM) + Tmz (100 μM)). Lane 1, control; lane 2, Tmz; lane 3, chrysin; lane 4, chrysin+Tmz. Bar graphs show the ratio expression of (B) phosphor-p38 MAPK/p38 MAPK and (C) phospho-ERK1/2/ERK1/2 in A172 and LN18 cell lines. Chrysin addition to Tmz significantly enhanced the activation of phospho-p38 MAPK and suppressed phospho-ERK1/2 in both cell lines compared to the Tmz-treated group. The JESS image blot was cropped from the whole blot according to the proteins. Values are S.E.M from three independent biological experiment (n=3), where *p <0.05, **p <0.01 are significant versus control and #p <0.05 is significant against Tmz-treated group.

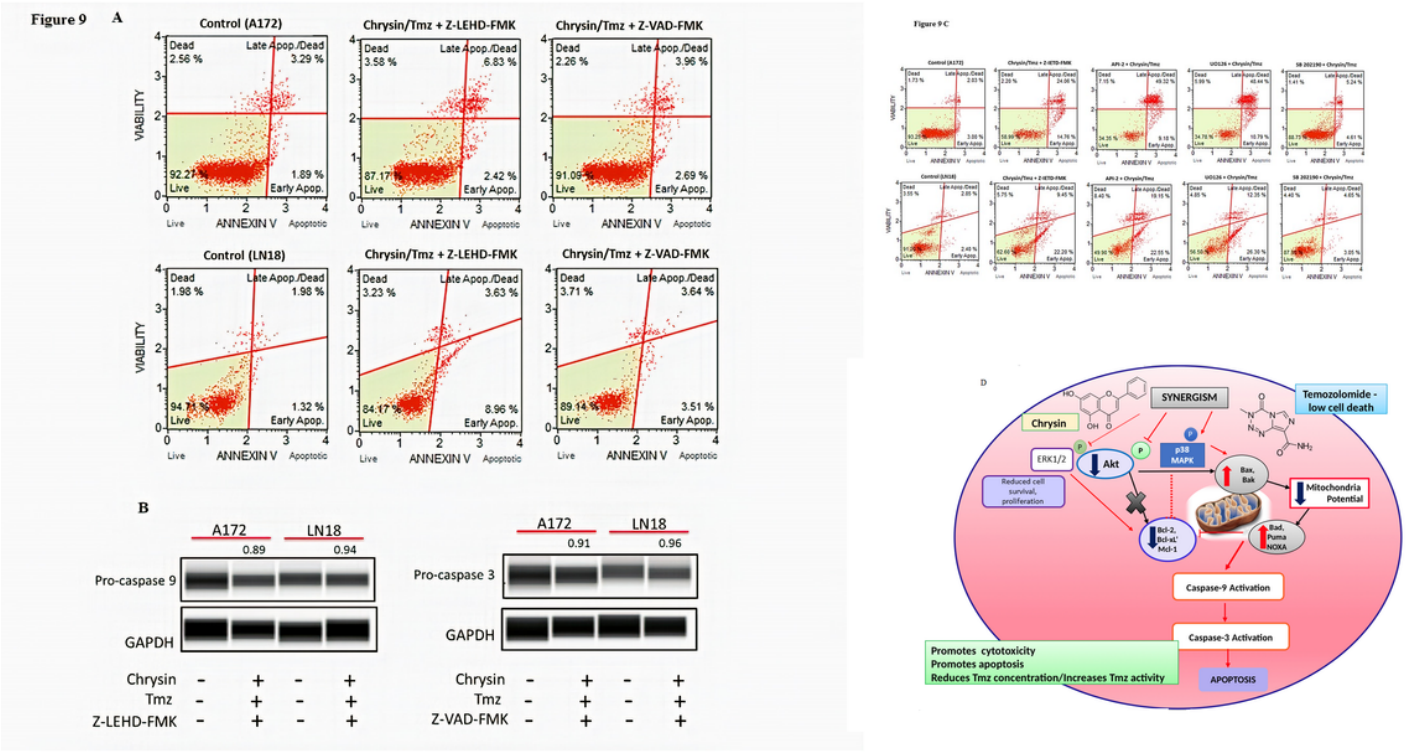

Figure 9

Addition of caspase-9 inhibitor (Z-LEHD-FMK, 2 μM) and caspase-3 inhibitor (Z-VAD-FMK, 5 μM) for 2 h suppressed chrysin ability to enhance Tmz-induced apoptosis as shown by inhibition of (A) phosphatidylserine externalization and (B) high procaspase-9 and -3 levels in both cell lines. The JESS image blot was cropped from the whole blot according to the proteins. (C) Pretreatment with Z-IETD-FMK did not suppress apoptosis in both A172 and LN18 cells, while API-2 (10 μM), U0126 (10 μM) promoted apoptosis, and SB 202190 (10 μM) inhibited apoptosis following treatment with a combination of chrysin and Tmz. Values are S.E.M from three independent biological experiments (n=3).

Supplementary Files

This is a list of supplementary files associated with this preprint. Click to download.

- SupplementaryInformationChrysinRAWIMAGESJESS.pdf